Temperature-independent ferromagnetic resonance shift in Bi-doped YIG garnets through magnetic anisotropy tuning

Diane Gouéré,[1,*] Hugo Merbouche,[1] Aya El Kanj,[1] Felix Kohl,[1] Cécile Carrétéro,[1] Isabella Boventer,[1] Romain Lebrun,[1] Paolo Bortolotti,[1] Vincent Cros,[1] Jamal Ben Youssef,[2] and Abdelmadjid Anane[1,†]

[1]*Unité Mixte de Physique CNRS, Thales, Université Paris-Saclay, 91767, Palaiseau, France*

[2]*Lab-STICC, UMR 6285 CNRS, Université de Bretagne Occidentale, 29238, Brest, France*

(Received 25 March 2022; revised 8 July 2022; accepted 20 September 2022; published 14 November 2022)

Thin garnet films are becoming central for magnon-spintronics and spin-orbitronics devices as they show versatile magnetic properties together with low magnetic losses. These fields would benefit from materials in which heat does not affect the magnetization dynamics, an effect known as the nonlinear thermal frequency shift. In this study, low-damping Bi substituted iron garnet (Bi:YIG) ultrathin films have been grown using pulsed laser deposition. Through a fine-tuning of the growth parameters, the precise control of the perpendicular magnetic anisotropy allows to achieve a full compensation of the dipolar magnetic anisotropy. Strikingly, once the growth conditions are optimized, varying the growth temperature from 405°C to 475°C as the only tuning parameter induces the easy axis to go from out of plane to in plane. For films that are close to the dipolar compensation, ferromagnetic resonance measurements yield an effective magnetization $\mu_0 M_{\text{eff}}$ (T) that has almost no temperature dependence over a large temperature range (260 to 400 K) resulting in an anisotropy temperature exponent of 2. These findings put the Bi:YIG system among the very few materials in which the temperature dependence of the magnetic anisotropy varies at the same rate as the saturation magnetization. This interesting behavior is ascribed phenomenologically to the sizable orbital moment of Bi^{3+}.

DOI: 10.1103/PhysRevMaterials.6.114402

I. INTRODUCTION

The recent discoveries in the field of insulating spintronics [1] have triggered an interest in the growth of ultrathin insulating film based on garnets [2]. The ultrafast magnetic domain walls (DWs) driven by spin-orbit torques in Bi-doped YIG films [3] ($Bi_xY_{3-x}Fe_5O_{12}$) as well as the coherent emission of spin waves (SWs) [4] has made such materials a favorable ground for new physical phenomena to be explored. Even though garnets have been investigated since the 1960s, the emergence of new growth approaches such as pulsed laser deposition (PLD) and off-axis sputtering [5] has proven that garnet ultrathin films can possess dynamical properties comparable to that of micrometer-thick films traditionally grown using liquid-phase epitaxy [6]. Interface transparency to pure spin currents that take place in adjacent heavy-metal layers (most often Pt) has allowed for efficient modulation of the SW lifetime through the dampinglike spin-orbit torque [7]. For instance, a fivefold increase of the SW attenuation length in 20-nm-thick YIG films has been observed and even auto-oscillations of the magnetization have been reached [8]. Nevertheless, the required electrical current flow for the generation of the torques in Pt also induces a Joule heating in the Pt/YIG bilayers. As a result, detrimental effects on the spin-wave spectrum appear, since heating-induced reduction of the saturation magnetization in turn generates a self-localization of the induced magnetization dynamics that inhibits SW emission and propagation [9]. This nonlinear frequency shift is reminiscent, even if the physical origin is different, of the soliton formation in all-metallic spin-Hall nano-oscillators [10]. A solution to this issue has been proposed using the out-of-plane magnetic anisotropy of $Bi_xY_{3-x}Fe_5O_{12}$ system [11]. In parallel to these lines of investigations, the study of spin-orbit torque-induced magnetic motion of DW in garnets thin films (such as Tm_3Fe_5O or $Bi_xY_{3-x}Fe_5O_{12}$) has pointed out the existence of a weak, but necessary, interfacial Dzyaloshinskii-Moriya interaction [12]. The $Bi_xY_{3-x}Fe_5O_{12}$ system hence appears as being the most versatile material platform as it combines tunable magnetic anisotropy and ultralow magnetic losses [13]. A precise control of this system will eventually lead to practical magnon-spintronics devices that could perform, for instance, in the static regime for memory application or in the dynamical regime for spin waves based information processing.

Up to now there are no reports establishing a clear correlation between growth parameters and magnetic anisotropy of doped garnets. Indeed, the magnetic anisotropy parameter for garnets, which is of importance for magnon-spintronics applications, is more usually tuned by extrinsic approaches such as the nature of the substrate, the nature of the dopant atom, or the content of the dopant atom [5,6,13]. In this study, we investigate the temperature dependence of the magnetic anisotropy of low-loss Bi-substituted thin-YIG films grown by PLD. First, the growth of thin films with optimal structural and magnetic properties has been optimized. Then, we show that by tailoring the growth temperature and only the growth

*diane.gouere@cnrs-thales.fr

†madjid.anane@universite-paris-saclay.fr

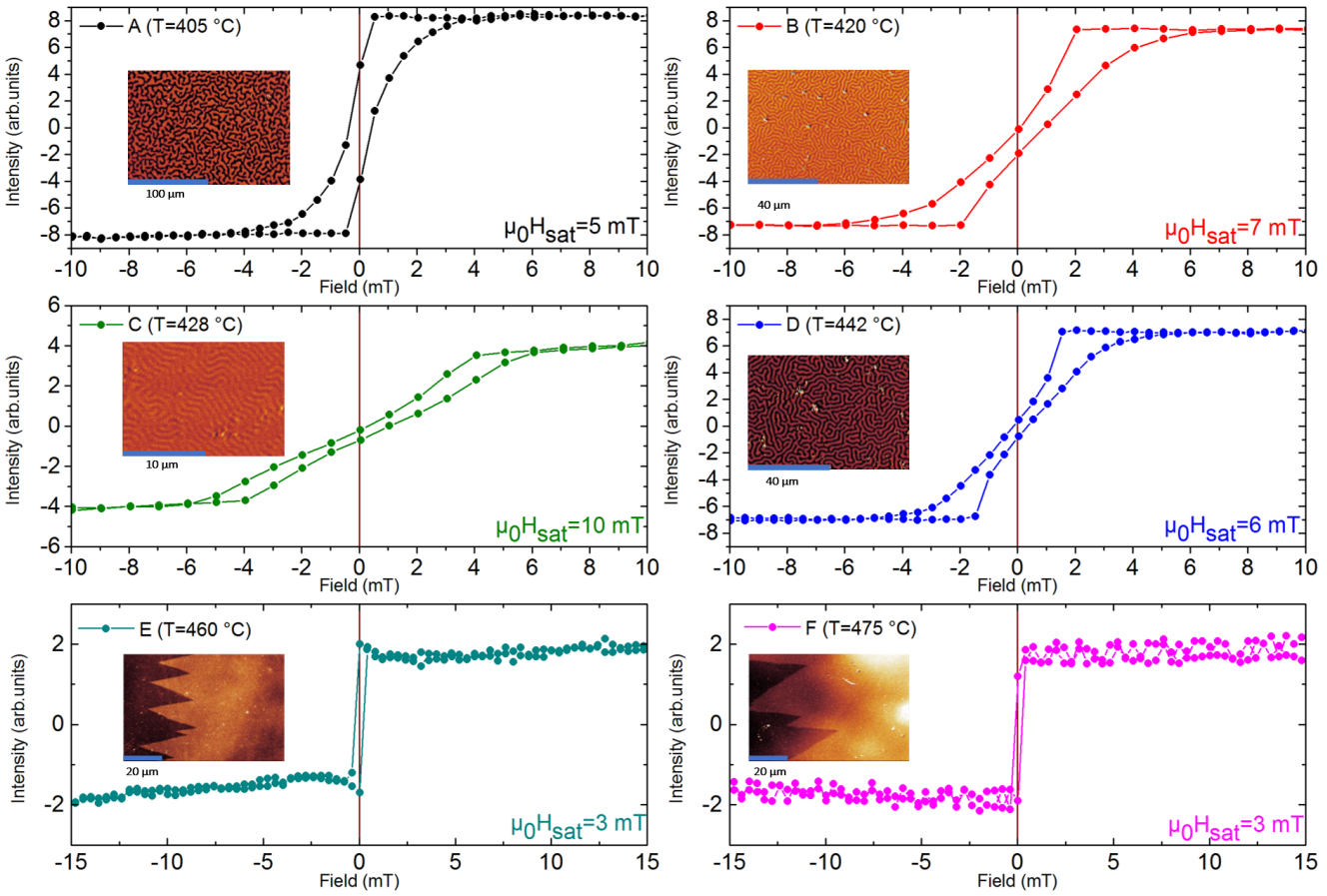

FIG. 1. MOKE measurements in polar mode (A, B, C, and D) and in the pure-transversal mode (E and F) for the 22-nm-thick Bi : YIG//sGGG films. Films grown between 405°C and 442°C have meander-like domain structure at remanance and an out-of-plane easy-magnetization axis. Films E and F grown at 460°C and 475°C are in-plane magnetized as evidenced by in-plane hystersesis cycles and the in-plane domains having characterestic zigzag boundaries. The saturation field is also indicated.

temperature, the film magnetic anisotropy can be tuned from out of plane to in plane, yielding a ferromagnetic resonance (FMR) frequency's temperature shift that is also tunable. We demonstrate that the FMR response can be finely adjusted and that we can even reach the conditions for which no temperature dependence on a large temperature range (260 to 400 K) is observed. This provides a route for material properties engineering to solve a long-standing issue of SW devices that up to now needed temperature regulation to perform correctly. By using suitable Bi:YIG, such devices can be made much more compact and less bulky by relieving the temperature stability constraints. Furthermore, temperature-independent magnetization dynamics will be instrumental for the development of future spin-orbitronics- and magnonics radio-frequency processing devices.

II. EXPERIMENTS

Thin films have been grown with a PLD process using a tripled-frequency YAG laser ($\lambda = 355$ nm) pulsed at 2.5 Hz. We use (111)-oriented substituted-Gd_3Ga_5O (sGGG) substrate and a single $Bi_1Y_2Fe_5O_{12}$ (Bi:YIG) target. The lattice parameters are $a = 12.497$ Å for the sGGG substrate and $a = 12.45$ Å for the Bi:YIG target. The laser fluence (1.3 J cm^{-2}), target-substrate distance (44 mm), oxygen pressure, growth rate, and all the other growth parameters have first been optimized. The oxygen pressure was set at 0.26 mbar during the growth process and Bi:YIG films were grown at temperatures ranging from 405°C to 475°C at a growth rate of 0.41 Å s^{-1}. Note that this temperature range is lower than what most studies report for the growth of garnets. Going from YIG, for which the growth temperature is reported to be superior to 650°C, to Bi:YIG has indeed an effect on the value of the optimal growth temperature. To preserve 2D-like reflection high-energy electron diffraction patterns, the growth temperature needs to be lowered.

The films' thicknesses have been determined by x-ray reflectivity and the structural characterizations have been performed by x-ray diffraction (XRD) using a five-axis Empyrean Panalytical setup with a Kα_1 monochromator ($\lambda = 1.540$ 56 Å). The static magnetic properties have been characterized by magneto-optical Kerr effect (MOKE) measurements with a magnetic field applied perpendicular or parallel to the film plane. In addition, we employ the "polar mode" to image the domain configuration for our samples with perpendicular magnetic anisotropy (PMA) and the "pure transversal mode" for films with in-plane easy-magnetization axis. The characterization of the magnetization dynamics has

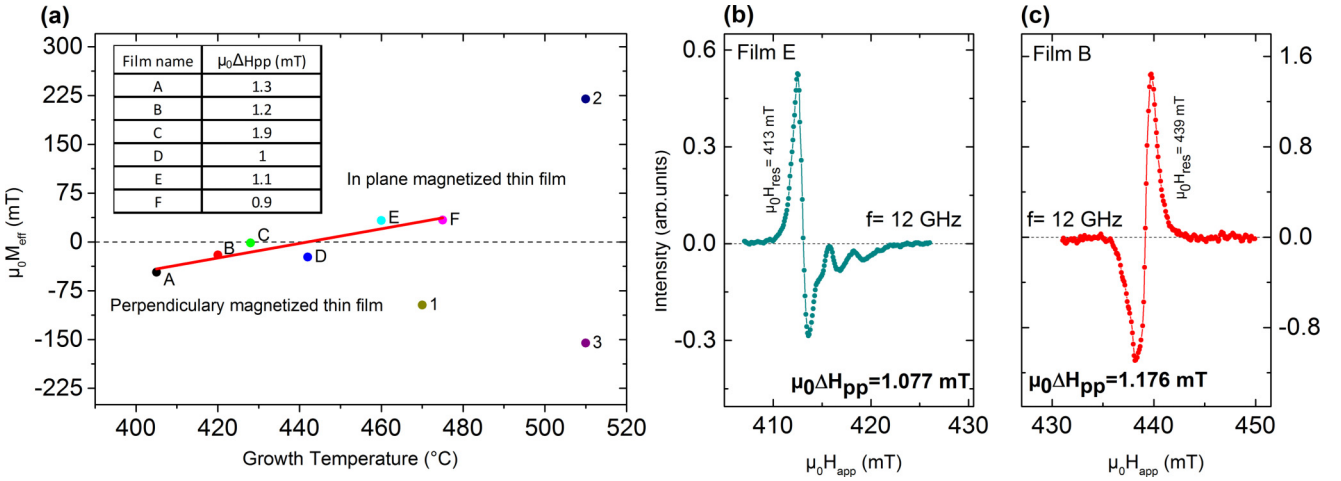

FIG. 2. Room-temperature FMR measurements in the in-plane field configuration. (a) Effective magnetization obtained through fitting to the Kittel formula [Eq. (1)] is ploted as a function of the growth temperature. The red line is a guide for the eye for the present series of six films (A, B, C, D, E, and F). Note the quasilinear temperature dependence of the effective magnetization that is negative for films with out-of-plane easy magnetization axis (A, B, C, and D) and positive for films with in-plane easy-magnetization axis (E, F). The linewidth at 12 GHz corresponding to the broadband FMR measurements is reported as an inset. Films labeled 1, 2, and 3 correspond to Bi:YIG films with larger effective magnetizations obtained either by changing the Bi content (1 and 2) or by changing the laser power (3). (b), (c) FMR absorption spectra for films E and B showing the lower resonance field for in-plane magnetized films.

been done using broadband FMR with frequencies ranging from 4 up to 40 GHz. The FMR measurements have been performed between 260 and 400 K in order to probe the temperature dependence of the magnetic properties.

All the elaborated films have a thickness of 22 ± 2 nm with a typical root-mean-square (rms) roughness of 0.4 nm over $5 \times 5\ \mu m^2$ (see Ref. [14]). The present study focuses on a series of six films in which a clear correlation is established between the growth temperature and the temperature dependence of the magnetic properties, such as magnetic anisotropy, effective magnetization, and nonlinear frequency shift. We use the Kerr effect to record the hysteresis cycle of the films. In Fig. 1, we show that films A to D grown at the lowest temperatures ($400\ ^\circ C < T_{growth} < 440\ ^\circ C$) exhibit an out-of-plane easy-magnetization axis with characteristic loop shapes and low saturation fields (< 10 mT). Insets of the polar-Kerr images confirm the uniaxial magnetic anisotropy; they show meander-like domains after demagnetization with characteristic domain size that decreases when increasing the growth temperature. For films E and F grown at higher temperature ($T_G = 460\ ^\circ C$ and $T_G = 475\ ^\circ C$) the hysteresis cycles have been obtained using an in-plane magnetic field in the pure transversal-Kerr mode, as their saturation in the polar field configuration is reached at much higher magnetic fields than films A–D. These films E and F have an in-plane easy-magnetic axis and, as shown by the insets in Fig. 1, highly contrasted in-plane domains with zigzag boundaries. These results indicate that modifying the growth temperature alone allows changing the PMA. Easy-magnetization axis is found to switch from out of plane to in plane at $T_G \approx 450\ ^\circ C$.

To characterize the magnetic anisotropy more precisely, we use broadband FMR in the field-in-plane configuration. Measurements have been performed from 4 to 20 GHz at room temperature. The Kittel formula is used to extract the value of the effective magnetization defined as $M_{eff} \stackrel{def}{=} M_s - H_u$, where M_s is the saturation magnetization and H_u is the uniaxial out-of-plane anisotropy field. The frequency dependence (f_{res}) of the FMR resonance field (H_{res}) is fitted for each film to

$$f_{res} = \mu_0 \gamma \sqrt{H_{res}(H_{res} + M_{eff})}, \quad (1)$$

where γ is the electron gyromagnetic ratio, fixed to its free-electron value, 28 GHz/T.

In Fig. 2(a), we show that the room-temperature effective magnetization ($\mu_0 M_{eff}$) for Bi-doped YIG thin films can vary over hundreds of mT (from −155 to 220 mT) when the target composition, the substrate, the growth temperature, the laser fluence, and the oxygen pressure are varied [13] (films labeled 1, 2, and 3). However, for the samples of interest here, labeled from A to F, we kept all parameters constant except for the growth temperature indicated on the x axis (Table I). It is observed for these films that the effective magnetization value changes within a much smaller range (from −46 to +33 mT) and increases almost linearly with T_G (the red line is a guide for the eye). Films grown below $T_G = 450\ ^\circ C$ have a negative effective magnetization. For films E and F, the effective magnetization is positive. The compensation ($M_{eff} = 0$) for which we observe the out-of-plane to in-plane spin reorientation transition is reached for $T_G \approx 428\ ^\circ C$ ($\mu_0 M_{eff} = -1.5$ mT). These results obtained by FMR are hence consistent with those obtained by Kerr imaging shown in Fig. 1: only films that show meander domains and out-of-plane easy-magnetization axis have negative effective magnetizations. The inset in Fig. 2(a) displays the peak-to-peak resonance linewidth values of films A to F. Note that the Gilbert damping parameters are comparable for all films and is about $\alpha = 7 \times 10^{-4}$ at room temperature. Optimization in the measurement geometry could eventually lead to a lower value such that for that of film F: $\alpha = 4 \times 10^{-4}$

TABLE I. Calculated magnetoelastic anisotropy constant (K_{MO}) for films grown between 405°C and 475°C, all other growth condition being identical. Deduced relaxed cell parameter(a_0) is given.

Film	Laser fluence (J cm^{-2})	Growth temperature (°C)	Growth rate (Å s^{-1})	Thickness (nm)	a_0 (nm)	K_{MO} (J m^{-3})
A		405				
B		420				
C	1.3	428	0.41	22	1.245	4560
D		442				
E		460				
F		475				

(see Ref. [14]). The absorption FMR spectra of films E [blue, Fig. 2(b)] and B [red, Fig. 2(c)] are reported for $f = 12$ GHz: both the peak-to-peak linewidth ($\mu_0\Delta H_{pp}$) and the resonance field ($\mu_0 H_{res}$) are indicated. We note that the resonance fields are shifted from $\mu_0 H_{res} = 413.1$ mT to $\mu_0 H_{res} = 439.2$ mT when the growth temperature decreases by 40 °C. Moreover, the resonance fields are lower (respectively, higher) than the expected resonance field $\mu_0 H_{res}(M_{eff} = 0) = 428.6$ mT calculated using Eq. (1) for compensated thin films. The growth temperature thus appears as a control knob for fine-tuning of the perpendicular magnetic anisotropy in a continuous way.

In order to obtain a more thorough characterization of the perpendicular magnetic anisotropy properties, FMR measurements from 5 to 40 GHz have been performed in an extended range of temperature (from 260 to 400 K). These measurements were done for thin films A–F, but also for films reported in Fig. 2(a) (films 1, 2, and 3). These films are presented to illustrate the extent to which the effective magnetization can vary in the Bi:YIG system; they have been grown using a different set of growth parameters (see Table II). In Fig. 3(a), we show effective magnetization as a function of the measurement temperature (T_{meas}) for thin films 1 and 3 with strong out-of-plane anisotropy. At $T_{meas} = 260$ K, $\mu_0 M_{eff}$ values are -156 and -102 mT, respectively. As reported in Fig. 3(b), the effective magnetization gradually increases until $T_{meas} = 400$ K (to $\mu_0 M_{eff} = -127$ mT and $\mu_0 M_{eff} = -77$ mT, respectively). The opposite behavior is observed for film 2 (with in-plane anisotropy) for which $\mu_0 M_{eff}$ decreases from $+232$ mT at $T_{meas} = 260$ K to $+166$ mT at $T_{meas} = 400$ K. This range of variation is to be compared to what is measured on films C and F that are closer to compensation, for which $\mu_0 M_{eff}$ varies only by $+6$ and -6 mT between 260 and 400 K. We note that the absolute thermal shift value is comparable for films C and F ($+0.039$ and -0.046 mT K^{-1}, respectively). It is observed that films with the largest $|\mu_0 M_{eff}|$ values have large temperature dependence of their effective magnetization. But, the temperature independence of $|\mu_0 M_{eff}|$, observed for films C and F, can only be explained by a specific power law between M_s and K_u (see Sec. III and Ref. [14]). Absorption FMR spectra acquired at 260, 300, and 340 K are shown in Fig. 3(c) for the film closest to compensation (film C) for which the resonance field shift ($\mu_0\delta H_{res}$) in this range of temperature is only $\mu_0\delta H_{res} \approx +4$ mT. It is also observed that the absorption linewidth is sharper at $T_{meas} = 400$ K than at lower temperatures as usually seen in thin garnet films [15].

X-ray diffraction has been used to investigate the structural properties of the Bi:YIG thin films. Inset in Fig. 4 displays the entire diffraction spectra (2θ angle varies from 10° to 130°) of film E in which several orders of diffractions are observed. The ones associated with sGGG substrate are identified for (444) and (888) together with forbidden reflections (222) and (666). We observe a systematic shoulder on the side of (444) and (888) peaks that is present even on the bare substrate originating, most probably, from a secondary sGGG phase. As shown in Fig. 4, the substrate's (888) diffraction peak is at $2\theta_{888} = 117.3°$ and its shoulder $2\theta_{888} = 117.7°$; Bi:YIG films diffract at $2\theta_{444} = 50.8°$ and $2\theta_{888} = 118.5°$. Diffraction spectra of thin films grown between $T_G = 405$ °C and $T_G = 475$ °C are plotted in the main panel of Fig. 4; $2\theta_{888} = 118.5°$ corresponds to a pseudocubic out-of-plane lattice constant of 1.242 nm. The relaxed Bi_1Y_2IG unit-cell parameter is expected to be 1.245 nm (against 1.249 nm for sGGG). As a consequence the $2\theta-\omega$ scan points toward tensile-strained Bi:YIG films at all growth temperatures. It is shown that the diffraction peaks of all films perfectly overlap, leading to a growth-temperature independent strain for Bi:YIG thin films. The identical shape of the films' peaks also indicated that the

TABLE II. Growth parameters of thin films 1, 2, and 3 compared with the one of films A and F of the study. The main difference is the laser fluence varying from 1 to 1.7 J cm^{-2}.

Film	Chemical composition	Growth temperature (°C)	O_2 pressure (mbar)	Thickness (nm)	Laser fluence (J cm^{-2})
1	Bi_1-YIG//sGGG	470		21	1.6
2	$Bi_{0.7}$-YIG//GGG	510		23	1.7
3	Bi_1-YIG//sGGG	510	0.25	25	1
A	Bi_1-YIG//sGGG	405		22	1.3
F	Bi_1-YIG//sGGG	475		22	1.3

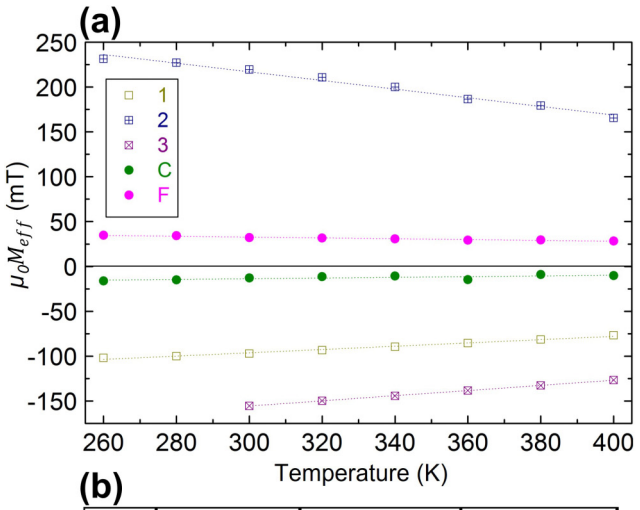

(b)

Film	Thermal Shift (mT/K)	$\mu_0 M_{eff}$ (mT) (260 K)	$\mu_0 M_{eff}$ (mT) (400 K)
1	0.18	-102	-76.9
2	-0.48	231.5	165.6
3	0.29	-155.5	-126.9
C	0.039	-16.18	-10.33
F	-0.046	34.59	28.11

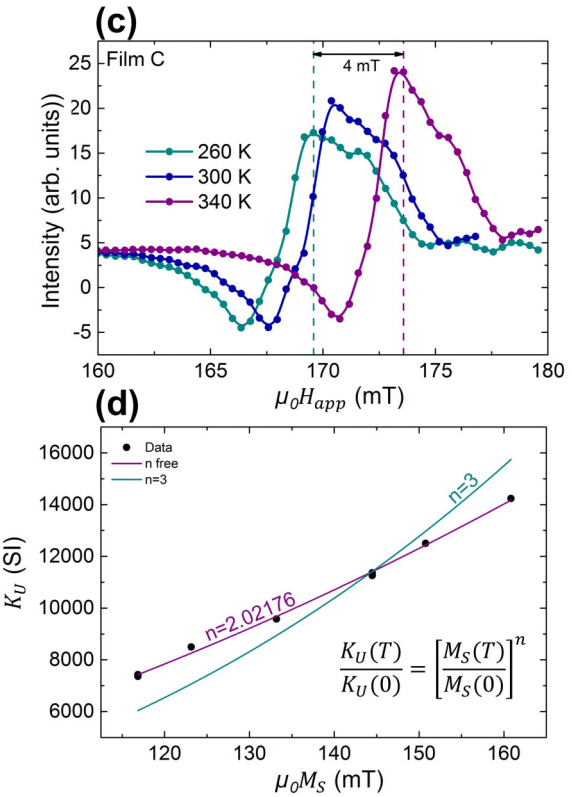

FIG. 3. Temperature dependence of the FMR measurements. (a) Effective magnetization is ploted as a function of the measurement temperature for films (C, F) of the study and three other films (1–3). For films with large effective magnetizations (1, 2, and 3) we observe a significant variation of its value when sweeping the measurement temperature, whereas (b) for films with much smaller effective magnetization (C, F) the temperature dependence is much smaller. (c) FMR absorption spectra for film C at three measurement temperatures at 5 GHz. The shift in the resonance field does not exceed 4 mT. (d) Inferred dependence of the out-of-plane anisotropy constant as a function of the saturation magnetization, including a fit which corresponds to an anisotropy exponent $n = 2$.

Bi content is constant among all films. The presence of Laue fringes at the (444) reflection is reminiscent of a pseudomorphic growth.

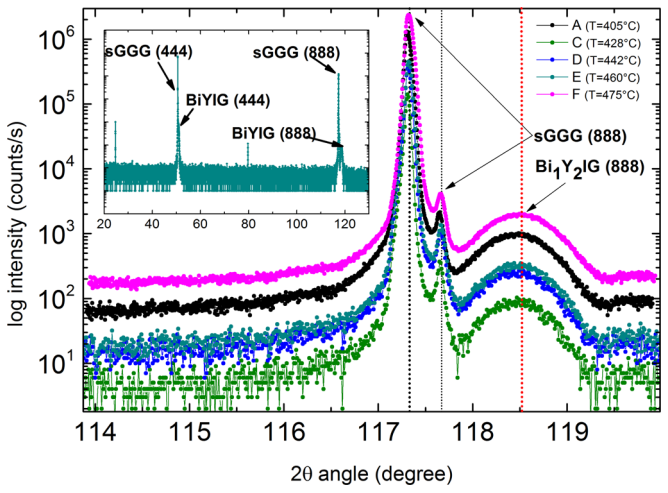

FIG. 4. $\theta-2\theta$ XRD spectra for Bi : YIG//sGGG. The main panel (with several films grown between 405 °C and 475 °C) in which (888) reflections show that the out-of-plane interlayer distance is identical for all films (curves have been offset for clarity). The inset displays a typical XRD pattern in 10°–130° range. No parasitic phase is observed.

III. DISCUSSION

One of the important results is that the magnetic anisotropy in the Bi:YIG system has two peculiarities. First, it can be finely tuned by the variation of the growth temperature. Second, its temperature dependence has a nonusual behavior in the vicinity of the dipolar compensation ($\mu_0 M_{\text{eff}} \approx 0$). In Bi-doped YIG the out-of-plane magnetic anisotropy has two origins: a magnetoelastic and a growth-induced term. The former results from epitaxial strain, for which the pseudomorphic in-plane elastic deformation yields either a negative or a positive magnetostrictive effect. For garnets deposited along the (111) axis, the magnetostrictive parameter (λ_{111}) is negative. A compressive strain favors in-plane magnetic anisotropy, while a tensile strain favors an out-of-plane easy-magnetization axis. In this study with a doping level of $x = 1$ ($Bi_xY_{3-x}Fe_5O_{12}$) and the sGGG substrate, we are in the former case, i.e., a tensile strain as the relaxed parameter (a_0) of Bi:YIG is smaller than that of the substrate. Hence, using the magnetoelastic theory, the out-of-plane misfit $\Delta a = a_{\text{sub}} - a_0$ (where a_{sub} is the lattice parameter of the substrate) is positive and yields a positive magnetoelastic anisotropy constant (K_{MO}) [16,17]:

$$K_{\text{MO}} = -\left[\frac{3}{2} \times \frac{E}{1+\mu} \times \left(\frac{\Delta_a}{a_0}\right) \times \lambda_{111}\right], \qquad (2)$$

$$\text{and } a_0 = \left[\frac{(a_{\text{film}}^{\perp} - a_{\text{sub}})}{1+\mu} \times (1-\mu) + a_{\text{sub}} \right], \qquad (3)$$

where $a_{\text{film}}^{\perp} = 1.242$ nm is the experimentally obtained out-of-plane lattice parameter, $E = 2.055 \times 10^{11}$ J m^{-3} and $\mu = 0.29$ are the Young modulus and the Poisson coefficient, respectively, and $\lambda_{111} = -5.0575 \times 10^{-6}$ is the magnetostrictive parameter [18,19]. Considering the XRD measurements performed on the Bi:YIG thin films, we calculated $a_0 = 1.245$ nm, $\Delta_a = 4.7 \times 10^{-3}$ nm and $K_{\text{MO}} = 4.56 \times 10^3$ J m^{-3},which favors an out-of-plane anisotropy. This value of K_{MO} is constant for all films of the study (A to F) as no change in the (888) diffraction peak is observed (see Fig. 4). For Bi:YIG thin films, the film's saturation magnetization (M_S) has been measured and its value is $M_S = 116$ kA m^{-1} ($\mu_0 M_S = 145.8$ mT) as previously reported by Lin *et al.* [20]. Note that this value is lower than that of undoped YIG thin films for which $M_S = 140$ kA m^{-1}. We can then deduce the magnetoelastic anisotropy field: $\mu_0 H_{\text{MO}} = \mu_0 \frac{2 K_{\text{MO}}}{M_S} = 98$ mT. This value is roughly 2/3 of $\mu_0 M_S$, alone it is yet far from sufficient to overcome the shape anisotropy. One needs to consider an extra term introduced five decades ago by Callen [21], known as the growth-induced anisotropy. It arises from the preferential occupation by Bi atoms of nonequivalent dodecahedral sites of the unit cell resulting in a symmetry lowering along the growth direction. This term contributes to the magnetic free energy of the system as $K_{\text{growth}} \sin^2\theta$, where θ is the polar angle relative to surface normal and K_{growth} the associated anisotropy constant. K_{growth} is positive under either a compressive or a tensile strain. In the present case, the fact that a vanishing effective magnetization is found implies that K_{growth} is of the same order than K_{MO}. Hence, the sum of both contributions compensates the dipolar term, whereas the cubic magnetic anisotropy is more than an order of magnitude smaller [16] and can be neglected at first order.

Our first main observation is the correlation between T_{growth} and the magnetic anisotropy. The relevant question is thus to identify which one of the anisotropy terms is varying with the growth temperature (T_{growth}). From x-ray diffraction, we obtain that the (888) diffraction peak remains identical for all films. Assuming a pseudomorphic growth for films A to F, we conclude that the relaxed cell parameter (a_0) is identical for all films. This has two consequences: (i) the Bi content and (ii) the strain state are identical for films A to F. We can therefore discard any significant variation of the magnetoelastic anisotropy among these films. As a consequence the only remaining anisotropy term affected by T_{growth} is the growth-induced anisotropy. In fact, we deduce a very strong variation of K_{growth} that spans from 4327 to 667 J m^{-3} over a growth-temperature range of only 75 °C. Such a large effect of T_{growth} on K_{growth} is largely unexpected. We speculate that the effect of growth temperature is due to a change in the Bi atoms' distribution over the nonequivalent six dodecahedral sites [22]. Yet difficult to evidence experimentally, this explanation is supported by the fact that increasing T_{growth} induces a monotonic decrease of growth anisotropy as expected from entropy arguments.

The second main observation is that the effective magnetization can be tuned to be almost temperature independent over a wide temperature range for films close to dipolar compensation, yielding an FMR frequency that is stable within 100 MHz ($\Delta f \approx \frac{\gamma \times \Delta M_{\text{eff}}}{2}$) over a 140 K temperature range. As a comparison, pure YIG films grown by PLD with similar thickness exhibit about an order of magnitude larger frequency shift over the same temperature range. Such a temperature dependence of the effective magnetization is the second peculiarity of the films under investigation. To have this effect, having a small value of $|\mu_0 M_{\text{eff}}|$, yet necessary, is not the only condition. In the system under investigation, H_u and M_s should have the same temperature dependence to keep $|\mu_0 M_{\text{eff}}|$ constant. Callen and Callen have proposed the following power law to relate the temperature dependence of the anisotropy to the temperature dependence of the magnetization [23]:

$$\frac{K_u(T)}{K_u(0)} = \left[\frac{M_s(T)}{M_s(0)} \right]^n, \qquad (4)$$

where K_u is the uniaxial magnetic anisotropy, M_s the saturation magnetization, and n is an exponent that is related to the crystal symmetry. It has been predicted by Van Vleck and Zener to be $n = 3$ in case of uniaxial anisotropy [24,25]. In our case, for a film with vanishing effective magnetization, we observe that $M_{\text{eff}}(T) \approx 0$, i.e., $M_s(T) \approx H_u(T)$. The uniaxial anisotropy field is therefore equal to the saturation magnetization at first order for all explored temperatures (from 260 to 400 K). Using Eq. (4), the uniaxial magnetic anisotropy $K_u(T) = \frac{\mu_0}{2} M_s(T) \times H_u(T)$ is thus simply proportional to the square of the saturation magnetization. This corresponds to an exponent $n = 2$ over a temperature range spanning at least from 260 to 400 K, while the film's Curie temperature is expected to be 559 K. A similar exponent $n = 2$ has been found while plotting (T) as a function of (T) and fitting the slope with Eq. (4) [Fig. 3(d)] (see Ref. [14]). The authors want to stress here that such exponent is not expected by the theory that has been developed for many systems including garnets. As a matter of fact, many systems in the literature deviate from their theoretical n exponent (given for cubic or uniaxial anisotropy). Indeed interestingly, there are few systems that deviate from the standard value of $n = 3$ [26–28]. Chatterjee *et al.* found an exponent $n = 2.6$ for the $NiFe_2O_4$ system, Wang *et al.* found an exponent of $n = 1$ for $BaFe_{12}O_{19}$, after fitting experimental data. Thus, although the deviation of the existent model is then not specific to the Bi:YIG system, the explanation may still differ from one system to the other. However, a value of $n = 2$ has only been reported for ordered Pt-Fe alloys of $L1_0$ type where this specific temperature dependence has been ascribed to a two-ion anisotropy related to the induced moments on the Pt [29]. For our films, even if Bi^{+3} ions in Bi:YIG are not expected to carry a spin magnetic moment, $M1$-edge x-ray circular magnetic dichroism experiments have unambiguously revealed that Bi atoms bear a sizable orbital moment [30]. This explains the fact that we observe a significantly smaller magnetization saturation than that of YIG, confirming previous observations (as Vertruyen *et al.* [31]). Additionally, the presence of the orbital moment may also explain a two-ion–like magnetic anisotropy behavior in Bi:YIG that would then be related

to the complex [$5d$, $6p$] Bi orbitals hybridization with Fe. We hence conclude that our observations are resulting from two effects that are growth-induced anisotropy sensitivity to growth temperature and the magnetic state of bismuth. A first-principle investigation could give enlightening insights on the interlinks between these two effects, which is beyond this work.

IV. CONCLUSION

In conclusion, we show (i) how to finely tune the magnetic anisotropy in garnets and (ii) how to obtain a temperature-free variation of their uniform magnetization dynamics characteristics when achieving a vanishing effective magnetization while preserving a low damping ($\alpha \approx 7 \times 10^{-4}$). We explain these observations, based on the growth-induced anisotropy for the former and on the importance to consider bismuth orbital momentum for the latter. Growth-induced anisotropy is found to be very sensitive to growth temperature, whereas no significant effect is observed on the magnetoelastic anisotropy. The anisotropy temperature exponent is found to change with the anisotropy; its value is $n \sim 2$ when the out-of-plane anisotropy compensates the shape anisotropy. The practical implications of these findings for the field of magnonics and spin orbitronics are numerous. At first, they solve a long-standing issue of YIG-based radio-frequency devices [32] that most often need thermally regulated packaging. Given the much smaller thermal sensitivity of optimized Bi:YIG, such technical constraints can now be lifted and more compact and less power-hungry devices could be developed. Furthermore, we explain why using Bi:YIG has been very important for the physics of spin-orbit torque in magnonics, where Joule heating is unavoidable. Not only is compensating exactly the dipolar contribution necessary to avoid nonlinear effects such as nonlinear magnon-magnon interactions [4], but it is equally important to suppress any temperature dependence of FMR frequency to avoid spin-wave localization. As the only temperature-dependent term in Eq. (1) is the effective magnetization, for low-damping materials, such condition can be reached in Bi:YIG and as far as the authors are aware of, only in the Bi:YIG system. Finally, we provide perspectives on how magnons' dispersion relation can be engineered to have the desired temperature dependence. Such latitude might open a field for magnonics lenses where the magnetic medium has reconfigurable effective indexes for spin-wave optical elements [33].

ACKNOWLEDGMENTS

We acknowledge support from the Agence Nationale de la Recherche (ANR), ANR MARIN Grant No. ANR-20-CE24-0012. This project has received funding from the European Union's Horizon 2020 research and innovation program under the Marie Skłodowska-Curie Grant Agreement No. 861300. and under FET-Open Grant No. 899646 (k-NET), and as part of the "Investissements d'Avenir" program (Labex NanoSaclay, Reference No. ANR-10-LABX-0035 "SPiCY."

[1] Y. Kajiwara, K. Harii, S. Takahashi, J. Ohe, K. Uchida, M. Mizuguchi, H. Umezawa, H. Kawai, K. Ando, K. Takanashi, S. Maekawa, and E. Saitoh, Transmission of electrical signals by spin-wave interconversion in a magnetic insulator, Nature (London) **464**, 262 (2010).

[2] G. Schmidt, C. Hauser, P. Trempler, M. Paleschke, and E. T. Papaioannou, Ultra thin films of yttrium iron garnet with very low damping: A review, Phys. Status Solidi Basic Res. **257**(7), 1900644 (2020).

[3] L. Caretta, S. H. Oh, T. Fakhrul, D. K. Lee, B. H. Lee, S. K. Kim, C. A. Ross, K. J. Lee, and G. S. D. Beach, Relativistic kinematics of a magnetic soliton, Science **370**, 1438 (2020).

[4] V. E. Demidov, S. Urazhdin, A. Anane, V. Cros, and S. O. Demokritov, Spin-orbit-torque magnonics, J. Appl. Phys. **127**, 170901 (2020).

[5] J. Ding, C. Liu, Y. Zhang, U. Erugu, Z. Quan, R. Yu, E. McCollum, S. Mo, S. Yang, H. Ding, X. Xu, J. Tang, X. Yang, and M. Wu, Nanometer-Thick Yttrium Iron Garnet Films with Perpendicular Anisotropy and Low Damping, Phys. Rev. Appl. **14**, 014017 (2020).

[6] Y. H. Rao, H. W. Zhang, Q. H. Yang, D. N. Zhang, L. C. Jin, B. Ma, and Y. J. Wu, Liquid phase epitaxy magnetic garnet films and their applications, Chin. Phys. B **27**, 086701 (2018).

[7] A. Hamadeh, O. d'Allivy Kelly, C. Hahn, H. Meley, R. Bernard, A. H. Molpeceres, V. V. Naletov, M. Viret, A. Anane, V. Cros, S. O. Demokritov, J. L. Prieto, M. Muñoz, G. de Loubens, and O. Klein, Full Control of the Spin-Wave Damping in a Magnetic Insulator Using Spin-Orbit Torque, Phys. Rev. Lett. **113**, 197203 (2014).

[8] M. Evelt, V. E. Demidov, V. Bessonov, S. O. Demokritov, J. L. Prieto, M. Muñoz, J. Ben Youssef, V. V. Naletov, G. De Loubens, O. Klein, M. Collet, K. Garcia-Hernandez, P. Bortolotti, V. Cros, and A. Anane, High-efficiency control of spin-wave propagation in ultra-thin yttrium iron garnet by the spin-orbit torque, Appl. Phys. Lett. **108**, 20 (2016).

[9] V. E. Demidov, S. Urazhdin, G. de Loubens, O. Klein, V. Cros, A. Anane, and S. O. Demokritov, Magnetization oscillations and waves driven by pure spin currents, Phys. Rep. **673**, 1 (2017).

[10] T. Chen, R. K. Dumas, A. Eklund, P. K. Muduli, A. Houshang, A. A. Awad, P. Durrenfeld, B. G. Malm, A. Rusu, and J. Åkerman, Spin-torque and spin-Hall nano-oscillators, Proc. IEEE **104**, 1919 (2016).

[11] M. Evelt, L. Soumah, A. B. Rinkevich, S. O. Demokritov, A. Anane, V. Cros, J. Ben Youssef, G. de Loubens, O. Klein, P. Bortolotti, and V. E. Demidov, Emission of Coherent Propagating Magnons by Insulator-Based Spin-Orbit-Torque Oscillators, Phys. Rev. Appl. **10**, 041002 (2018).

[12] S. Ding, A. Ross, R. Lebrun, S. Becker, K. Lee, I. Boventer, S. Das, Y. Kurokawa, S. Gupta, J. Yang, G. Jakob, and M. Kläui, Interfacial Dzyaloshinskii-Moriya interaction and chiral magnetic textures in a ferrimagnetic insulator, Phys. Rev. B **100**, 100406(R) (2019).

[13] L. Soumah, N. Beaulieu, L. Qassym, C. Carrétéro, E. Jacquet, R. Lebourgeois, J. Ben Youssef, P. Bortolotti, V. Cros, and A. Anane, Ultra-low damping insulating magnetic thin films get perpendicular, Nat. Commun. **9**, 3355 (2018).

[14] See Supplemental Material at http://link.aps.org/supplemental/10.1103/PhysRevMaterials.6.114402 for more details on AFM, FMR, and explanations of the magnetic anisotropy exponent.

[15] N. Beaulieu, N. Kervarec, N. Thiery, O. Klein, V. Naletov, H. Hurdequint, G. De Loubens, J. Ben Youssef, and N. Vukadinovic, Temperature dependence of magnetic properties of a ultrathin yttrium-iron garnet film grown by liquid phase Epitaxy: effect of a Pt overlayer, IEEE Magn. Lett. **9**, 3706005 (2018).

[16] Lucile Soumah, *Pulsed Laser Deposition of Substituted Thin Garnet Films for Magnonic*, Ph.D, University Paris-Saclay (2019), https://www.theses.fr/2019SACLS042.

[17] P. Hansen and J. P. Krumme, Magnetic and magneto-optical properties of garnet films, Thin Solid Films **114**, 69 (1984).

[18] Jamal Ben Youssef, *Elaboration Par Epitaxie En Phase Liquide, Caracterisation et Etude Physique Des Filmsminces de Grenats Ferrimagnetiques Susbstitues Par Des Ions Bismuth*, Ph.D, University Paris VI (1989), https://www.theses.fr/1989PA066048.

[19] P. Hansen, C.-P. Klages, J. Schuldt, and K. Witter, Magnetic and magneto-optical properties of bismuth-substituted lutetium iron garnet films, Phys. Rev. B **31**, 5858 (1985).

[20] Y. Lin, L. Jin, H. Zhang, Z. Zhong, Q. Yang, Y. Rao, and M. Li, Bi-YIG ferrimagnetic insulator nanometer films with large perpendicular magnetic anisotropy and narrow ferromagnetic resonance linewidth, J. Magn. Magn. Mater. **496**, 165886 (2020).

[21] H. Callen, Growth-induced anisotropy by preferential site ordering in garnet crystals, Appl. Phys. Lett. **18**, 311 (1971).

[22] P. Novak, Contribution of $Fe3^{+}$ ions to the growth induced anisotropy in garnet films, Czech. J. Phys. B **34**, 1060 (1984).

[23] H. B. Callen and E. Callen, The present status of the temperature dependence of magnetocrystalline anisotropy, and the l$(L + 1)$ 2 power law, J. Phys. Chem. Solids **27**, 1271 (1966).

[24] J. H. Van Vleck, On the anisotropy of cubic ferromagnetic crystals, Phys. Rev. **52**, 1178 (1937).

[25] C. Zener, Classical theory of the temperature dependence of magnetic anisotropy energy, Phys. Rev. **96**, 1335 (1954).

[26] B. K. Chatterjee, C. K. Ghosh, and K. K. Chattopadhyay, Temperature dependence of magnetization and anisotropy in uniaxial $NiFe_2O_4$ Nanomagnets: Deviation from the Callen-Callen power law, J. Appl. Phys. **116**, 153904 (2014).

[27] J. Wang, F. Zhao, W. Wu, and G. M. Zhao, Unusual temperature dependence of the magnetic anisotropy constant in barium ferrite $BaFe_{12}O_{19}$, J. Appl. Phys. **110**, 10 (2011).

[28] G. Long, H. Zhang, D. Li, R. Sabirianov, Z. Zhang, and H. Zeng, Magnetic anisotropy and coercivity of Fe_3Se_4 nanostructures, Appl. Phys. Lett. **99**, 4 (2011).

[29] K. Inoue, H. Shima, A. Fujita, K. Ishida, K. Oikawa, and K. Fukamichi, Temperature dependence of magnetocrystalline anisotropy constants in the single variant state of l 10-type FePt bulk single crystal, Appl. Phys. Lett. **88**, 86 (2006).

[30] A. Rogalev, J. Goulon, F. Wilhelm, C. Brouder, A. Yaresko, J. Ben Youssef, and M. V. Indenbom, Element selective x-ray magnetic circular and linear dichroisms in ferrimagnetic yttrium iron garnet films, J. Magn. Magn. Mater. **321**, 3945 (2009).

[31] B. Vertruyen, R. Cloots, J. S. Abell, T. J. Jackson, R. C. da Silva, E. Popova, and N. Keller, Curie temperature, exchange integrals, and magneto-optical properties in off-stoichiometric bismuth iron garnet epitaxial films, Phys. Rev. B: Condens. Matter Mater. Phys. **78**, 094429 (2008).

[32] W. S. Ishak, Magnetostatic wave technology: A review, Proc. IEEE **76**, 171 (1988).

[33] M. Vogel, P. Pirro, B. Hillebrands, and G. Von Freymann, Optical elements for anisotropic spin-wave propagation, Appl. Phys. Lett. **116**, 262404 (2020).